

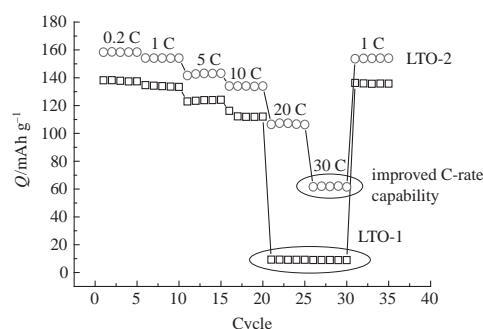
## Electrochemical performance of lithium titanate anode fabricated using a water-based binder

Ekaterina V. Shkreba, Svetlana N. Eliseeva, Rostislav V. Apraksin,  
Mikhail A. Kamenskii, Elena G. Tolstopjatova and Veniamin V. Kondratiev\*

Institute of Chemistry, St. Petersburg State University, 199034 St. Petersburg, Russian Federation.  
Fax: +7 812 428 6900; e-mail: vkondratiev@mail.ru

DOI: 10.1016/j.mencom.2019.01.036

A novel anode material based on  $\text{Li}_4\text{Ti}_5\text{O}_{12}$  prepared using the combination of poly-3,4-ethylenedioxythiophene/polystyrene sulfonate and carboxymethylcellulose for the conducting polymer binder was developed. The comparative study of this material with conventional polyvinylidene fluoride and with the conductive polymer binder by the cyclic voltammetry and galvanostatic charge–discharge methods revealed that the anode material modified with the conductive binder possesses superior properties in terms of higher specific capacity (increase up to 14%), improved high-rate capability, and life cycle stability of battery.



Lithium titanium oxide  $\text{Li}_4\text{Ti}_5\text{O}_{12}$  (LTO) is a promising anode material for the lithium ion batteries due to its extremely low lattice strain during the charge–discharge processes, reasonable specific capacity, and high rate capability.<sup>1–3</sup> However, concerning the stability issues, the conventional type of electrodes containing a polyvinylidene fluoride (PVDF) binder has shown irreversible surface morphology changes resulting in capacity losses and low life cycle.<sup>4–8</sup> Among common causes of degradation of electroactive materials are loss of electrical contacts, decrease in the efficiency of its utilization during charge–discharge cycles due to the formation of surface layers on grains.<sup>9</sup>

Several approaches have been proposed to improve the electrochemical performance of LTO materials,<sup>10–17</sup> e.g., a surface modification of LTO by  $\text{TiO}_2$  layers,<sup>11,12</sup> an application of conducting polymer such as polyaniline<sup>13,14</sup> or polythiophene layers,<sup>15,16</sup> and replacing the PVDF binder by a carboxymethylcellulose (CMC) one.<sup>17</sup> The influence of binder nature on the functional characteristics of electrodes has recently been intensively studied. The change in the nature of intergranular space, wherein the electrolyte is located, can greatly effect on the charge transfer conditions. Taking into account the reported results,<sup>18</sup> it can also be assumed that the effects of structural transformation of surface of LTO grains can be suppressed in the presence of poly-3,4-ethylenedioxythiophene/polystyrene sulfonate (PEDOT:PSS) and CMC polymers used.

Here we report on the high electrochemical performance of LTO-based anode with conductive binder PEDOT:PSS/CMC and their improved functional characteristics in comparison with PVDF-bound electrodes.<sup>†</sup>

<sup>†</sup>  $\text{Li}_4\text{Ti}_5\text{O}_{12}$  powder (<200 nm), PEDOT:PSS (1.3 wt%, aqueous dispersion), PVDF, and *N*-methylpyrrolidone (NMP) were purchased from Aldrich. CMC was obtained from MTI Corp. (USA). Conducting carbon black ‘Super P’ was purchased from Timcal Inc. (Belgium). Commercial battery electrolyte TCE918 was from Tinci Materials Technology Co. Ltd. (China). All reagents were used as received.

Figure 1(a) shows cyclic voltammograms of electrodes with a conventional PVDF binder (LTO-1) and with conductive binder PEDOT:PSS/CMC (LTO-2). At a potential scan rate of  $0.1 \text{ mV s}^{-1}$ , a pair of distinct redox peaks was observed for LTO-1 at the potentials of 1.82 and 1.41 V ( $\Delta E_p = 0.41 \text{ V}$ ) and for LTO-2 at the potentials of 1.68 and 1.45 V ( $\Delta E_p = 0.23 \text{ V}$ ). The observed pair of redox peaks is related to the redox transition of  $\text{Ti}^{4+}/\text{Ti}^{3+}$  in the LTO structure, followed by the intercalation of lithium ions [equation (1)].



The asymmetric voltammetric response for LTO-1 indirectly indicates the different conditions of kinetics of charge transfer during the oxidation–reduction cycles. Similar shape of CV curves for the conventional PVDF-bound LTO electrode has been reported previously.<sup>19</sup> The asymmetry of voltammetric response may be due to the lithium deintercalation proceeding

Two types of electrodes were prepared by mechanical mixing of components for 1 h until the slurry had become homogeneous. The LTO-1 electrodes contained  $\text{Li}_4\text{Ti}_5\text{O}_{12}$  (80 wt%), C (10 wt%), and PVDF (10 wt%) dissolved in NMP, while the LTO-2 electrodes contained  $\text{Li}_4\text{Ti}_5\text{O}_{12}$  (90 wt%), C (6 wt%), PEDOT:PSS (2 wt%), and CMC (2 wt%). All electrodes were cut into disks with the area of  $1.7 \text{ cm}^2$ , and the average mass material loading was about  $4–6 \text{ mg cm}^{-2}$ .

Electrochemical characterization of electrodes was conducted in standard two-electrode coin-type half cells (CR2032). The cells were assembled in an argon-filled glove box Unilab (USA). Cyclic voltammograms were recorded on Autolab PGSTAT 30 potentiostat/galvanostat (Eco-Chemie, Netherlands) in the range of potentials from 0.9 to 2.5 V at the potential scan rate of  $0.1 \text{ mV s}^{-1}$ . The electrochemical performance tests were carried out on an automatic galvanostatic charge–discharge battery cell test instrument (Neware Co., China) in the potential range between 1.0 and 2.5 V (vs.  $\text{Li}^+/\text{Li}$ ) at different current rates from 0.2 to 30 C at room temperature ( $20 \pm 2^\circ\text{C}$ ). The theoretical charge–discharge capacity of active material in the different electrodes was assumed as  $175 \text{ mAh g}^{-1}$ . All the reported capacity values were normalized by the total mass of electrodes excluding the current collector unless otherwise noted.

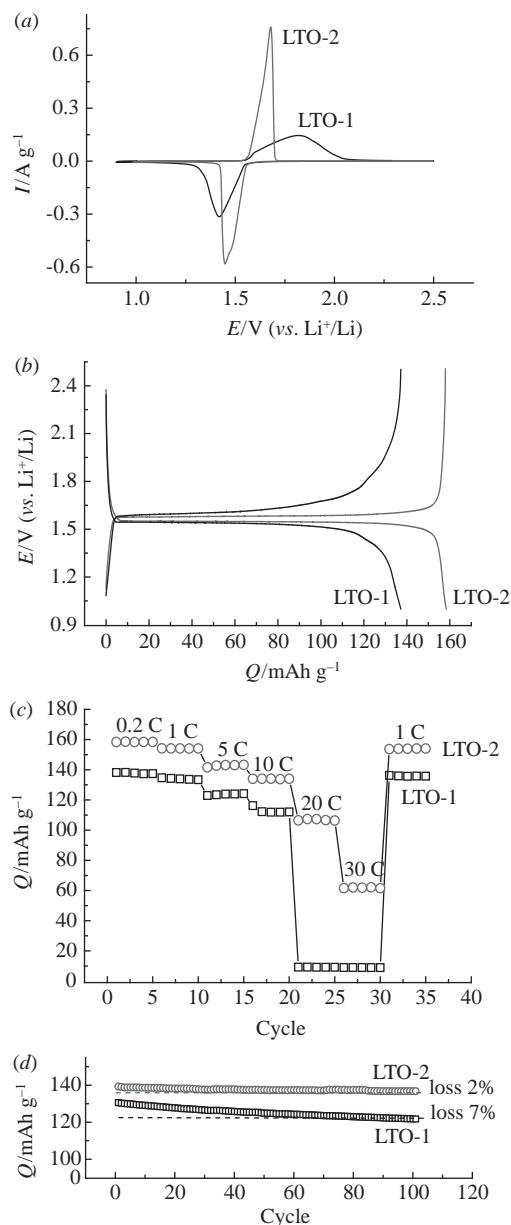


**Figure 1** (a) Cyclic voltammograms of LTO-1 and LTO-2 electrodes at the scan rate of  $0.1 \text{ mV s}^{-1}$ , (b) galvanostatic charge–discharge curves of LTO-1 and LTO-2 at  $0.2 \text{ C}$ , (c) discharge capacities of LTO-1 and LTO-2 at the different discharge current densities capacity vs. the cycle number, and (d) cycling performance of LTO-1 and LTO-2 electrodes at  $1 \text{ C}$  rate.

with greater kinetic difficulties as compared to the intercalation process.<sup>20,21</sup>

The cathode peak for LTO-2 located at the potential of  $1.45 \text{ V}$  corresponds to the discharge process, wherein the lithium ion is intercalated into the  $\text{Li}_4\text{Ti}_5\text{O}_{12}$  structure, while the anode peak (at  $E = 1.68 \text{ V}$ ) corresponds to the charge process, where the lithium ion is deintercalated from  $\text{Li}_7\text{Ti}_5\text{O}_{12}$ . For the LTO-2 electrode, the smaller difference between the peak potentials and the higher peak currents as compared to LTO-1 were observed. The acquired data indicate an improvement in the reversibility of electrode process in the case of the conductive polymer additive introduced, indicating a good reversibility of lithium intercalation processes during the phase transition between  $\text{Li}_4\text{Ti}_5\text{O}_{12}$  and  $\text{Li}_7\text{Ti}_5\text{O}_{12}$ .

The galvanostatic charge–discharge curves (at current density of  $0.2 \text{ C}$ ) for both types of electrodes in coin cells [Figure 1(b)] contain characteristic voltage plateaus at the potentials of about  $1.6 \text{ V}$ , corresponding to the lithium intercalation–deintercalation into the spinel structure.<sup>9</sup> In the LTO battery cell with Li cathode,

**Table 1** The specific capacities ( $\text{mAh g}^{-1}$ ) of LTO-1 and LTO-2 electrodes at different currents related to the total mass ( $Q_{\text{electrode}}$ ) and the mass of active material ( $Q_{\text{LTO}}$ ).

Current/C	LTO-1		LTO-2	
	$Q_{\text{electrode}}$	$Q_{\text{LTO}}$	$Q_{\text{electrode}}$	$Q_{\text{LTO}}$
0.2	137	171	157	174
1	135	169	154	171
5	124	155	143	159
10	112	140	134	149
20	10	13	108	120
30	9	11	62	69

the lithium deintercalation anode process corresponds to the discharge of lithium titanate. The specific capacities of the LTO-1 and LTO-2 electrodes at  $0.2 \text{ C}$  were  $137$  and  $158 \text{ mAh g}^{-1}$ , respectively. The coulombic efficiency of these electrodes was remaining stable and close to approximately  $100\%$  during their cycling up to  $100$  cycles, which indicates the complete reversibility of electrochemical lithium insertion process.

Charge–discharge curves for LTO-1 and LTO-2 electrodes were also recorded at the different discharge currents from  $0.2$  to  $30 \text{ C}$  in the voltage range of  $1.0$ – $2.5 \text{ V}$ . It was shown (Table 1) that the specific capacity of LTO-1 electrode dropped more significantly upon the increased current density than that of LTO-2 electrode [Figure 1(c)]. The LTO-2 demonstrated a remarkably better specific capacity ( $62 \text{ mAh g}^{-1}$ ) even at the current density of  $30 \text{ C}$  (see Table 1). Moreover, the increased difference between the potentials of charge and discharge plateaus was observed for LTO-1 electrode due to its higher ohmic resistance in comparison with the LTO-2 electrode.

After the measurements at current of  $30 \text{ C}$ , the additional repeated measurement was performed at the current of  $1 \text{ C}$ , and the capacities for the both types of electrodes returned to the same values at the current of  $1 \text{ C}$ . This indicates the reproducibility of observed values of discharge capacities, and consequently, the kinetic limitations should be considered as the main reason for the capacity drop at high discharge rates during recharging the LTO. Thus, the data obtained at higher discharge rates confirmed the assumption of decreased kinetic limitations in the case of LTO modification with PEDOT:PSS and CMC, as compared to the PVDF binder, and the smaller capacity drops at the higher current densities revealed the opportunity to increase the battery power via the application of this material.

Figure 1(d) shows the cycling performance of LTO electrodes at room temperature and the current density of  $1 \text{ C}$ . The capacity decay was about  $2\%$  after  $100$  cycles for LTO-2, whereas that for LTO-1 was about  $7\%$ .

The combined conductive polymer binder provides a partial or complete wrapping of LTO grains, which can more efficiently inhibit the interaction of active material with the electrolyte and side reactions without the hindering of lithium transport, thus reducing the degradation of LTO-2 as compared to the LTO-1. Taking into account the reported results,<sup>17</sup> one can also assume that the introduction of polymers (PEDOT:PSS and CMC) suppresses the effects of structural transformation on the LTO surface.

In summary, the simple approach to the fabrication of electrodes based on the commercially available LTO and the combination of conducting polymer PEDOT:PSS with carboxymethylcellulose as the binder was proposed, practically realized to result in the better electrochemical performance of developed LTO electrode as compared to the conventional PVDF-bound LTO electrode. The major functional characteristics of this novel electrode, especially high specific capacity and its maintenance at enhanced charge–

discharge currents, were markedly improved. Therefore, the proposed approach is efficient for the manufacture of electrodes possessing the increased practical capacity and power density and, consequently, for the production of commercial batteries. In addition, the employment of water-based conducting binder PEDOT:PSS/CMC instead of PVDF in toxic flammable solvent NMP is another advantage of our work due to the environmental compatibility.

This work was supported by the St. Petersburg State University (grant no. 26455158).

## References

- 1 B. Zhao, R. Ran, M. Liu and Z. Shao, *Mater. Sci. Eng. R.*, 2015, **98**, 1.
- 2 A. B. Yaroslavtsev, T. L. Kulova and A. M. Skundin, *Russ. Chem. Rev.*, 2015, **84**, 826.
- 3 C. P. Sandhya, B. John and C. Gouri, *Ionics*, 2014, **20**, 601.
- 4 K. Zaghbi, M. Simoneau, M. Armand and M. Gauthier, *J. Power Sources*, 1999, **81–82**, 300.
- 5 M. Armand and J. M. Tarascon, *Nature*, 2008, **451**, 652.
- 6 T.-F. Yi, L.-J. Jiang, J. Shu, C.-B. Yue, R.-S. Zhu and H.-B. Qiao, *J. Phys. Chem. Solids*, 2010, **71**, 1236.
- 7 M. V. Reddy, G. V. Subba Rao and B. V. R. Chowdari, *Chem. Rev.*, 2013, **113**, 5364.
- 8 M. Kitta, T. Akita and M. Kohyama, *J. Electrochem. Soc.*, 2015, **162**, A1272.
- 9 P. G. Bruce, B. Scrosati and J. M. Tarascon, *Angew. Chem. Int. Ed.*, 2008, **47**, 2930.
- 10 T. L. Kulova, Yu. M. Kreshchenova, A. A. Kuz'mina, A. M. Skundin, I. A. Stenina and A. B. Yaroslavtsev, *Mendeleev Commun.*, 2016, **26**, 238.
- 11 J. Wang, H. Zhao, Q. Yang, C. Wang, P. Lv and Q. Xia, *J. Power Sources*, 2013, **222**, 196.
- 12 T.-F. Yi, Z.-K. Fang, Y. Xie, Y.-R. Z and S.-Y. Yang, *ACS Appl. Mater. Interfaces*, 2014, **6**, 20205.
- 13 Z. He, L. Xiong, S. Chen, X. Wu, W. Liu and K. Huang, *Trans. Nonferrous Met. Soc. China*, 2010, **20**, s262.
- 14 D. Xu, P. Wang and R. Yang, *Ceram. Int.*, 2017, **43**, 7600.
- 15 X. Wang, L. Shen, H. Li, J. Wang, H. Dou and X. Zhang, *Electrochim. Acta*, 2014, **129**, 283.
- 16 Y. Liu, D. Tang, H. Zhong, Q. Zhang, J. Yang and L. Zhang, *RSC Adv.*, 2016, **6**, 95512.
- 17 B.-R. Lee and E.-S. Oh, *J. Phys. Chem. C*, 2013, **117**, 4404.
- 18 H.-C. Chiu, X. Lu, J. Zhou, L. Gu, J. Reid, R. Gauvin, K. Zaghbi and G. P. Demopoulos, *Adv. Energy Mater.*, 2016, **7**, 1601825.
- 19 B. Yan, M. Li, X. Li, Z. Bai, J. Yang, D. Xiong and D. Li, *J. Mater. Chem. A*, 2015, **3**, 11773.
- 20 W. K. Pang, V. K. Peterson, N. Sharma, J.-J. Shiu and S. Wu, *Chem. Mater.*, 2014, **26**, 2318.
- 21 L. Kavan, J. Procházka, T. M. Spitzler, M. Kalbáč, M. Zukalová, T. Drezen and M. Grätzel, *J. Electrochem. Soc.*, 2003, **150**, A1000.

Received: 6th July 2018; Com. 18/5632